

Spring 4-26-2024

Numerical Investigation to Produce a Fundamental Polygon

Elizabeth Sipes

Follow this and additional works at: <https://digitalcommons.murraystate.edu/honorstheses>



Part of the [Geometry and Topology Commons](#)

Recommended Citation

Sipes, Elizabeth, "Numerical Investigation to Produce a Fundamental Polygon" (2024). *Honors College Theses*. 234.

<https://digitalcommons.murraystate.edu/honorstheses/234>

This Thesis is brought to you for free and open access by the Student Works at Murray State's Digital Commons. It has been accepted for inclusion in Honors College Theses by an authorized administrator of Murray State's Digital Commons. For more information, please contact msu.digitalcommons@murraystate.edu.

Murray State University Honors College

HONORS THESIS

Certificate of Approval

Numerical Investigation to Produce a Fundamental Polygon

Elizabeth Sipes
May 2024

Approved to fulfill the
requirements of HON 437

Dr. Dubravko Ivansic, Associate Professor
Mathematics and Statistics

Approved to fulfill the
Honors Thesis requirement
of the Murray State Honors
Diploma

Dr. Warren Edminster, Executive Director
Honors College

Examination Approval Page

Author: Elizabeth Sipes

Project Title: Numerical Investigation to Produce a Fundamental Polygon

Department: Mathematics and Statistics

Date of Defense: April 26, 2024

Approval by Examining Committee:

(Dr. Dubravko Ivansic, Advisor)

(Date)

(Dr. David Gibson, Committee Member)

(Date)

(Dr. Omer Yayenie, Committee Member)

(Date)

Numerical Investigation to Produce a Fundamental Polygon

Submitted in partial fulfillment
of the requirements
for the Murray State University Honors Diploma

Elizabeth Sipes

May 2024

Abstract

There exist multiple types of geometry, differing in the postulates they are based on, and therefore the theorems and proofs that make up said geometry. Hyperbolic geometry differs from others by allowing there to exist multiple lines through a single point not on a given line, that are parallel to the given line. Every geometry has the idea of distance and isometries, distance preserving maps. By considering special collections of isometries called discrete groups, we can construct interesting surfaces, such as the torus and genus- g surface. The connection between the surface and the discrete group can be understood through the fundamental polygon, a polygon whose images by the isometries properly cover the plane R^2 or hyperbolic space D^2 . While there are a number of ways to construct a fundamental polygon, we numerically investigate the behavior of images of a line by the group of hyperbolic isometries to see if they can be used to construct a fundamental polygon.

Contents

1	Euclidean Geometry	1
2	The Torus and Groups	6
3	Hyperbolic Geometry and the D^2 Model	12
4	$4g$-gon and the Genus-g Surface	20
5	Computation Setup	22
6	Results	23
7	Conclusion	26

List of Figures

1	Example of equidistant points	2
2	Example of a translation	2
3	Reflection in the x-axis	3
4	Example of a rotation by 90°	4
5	Translation followed by a reflection (also known as a glide reflection	4
6	Fundamental polygon of a cylinder with horizontal translations	7
7	Fundamental region of a torus	8
8	Process of forming a torus from the fundamental polygon	8
9	Fundamental polygon of Klein bottle	9
10	Fundamental polygon of Mobius strip	10
11	Translates of line with slope $\sqrt{2}$	11
12	Translations of two lines with rational slope, forming a grid	11
13	Example of parallel postulate: Point P is not on the line m, and n is the only line going through point P parallel to line m	12
14	Parallel postulate in hyperbolic geometry: Through the point P not on the given line l, there exists two lines, m and n, going through point P parallel to line l	13
15	Parallel lines in Euclidean geometry vs hyperbolic geometry	13
16	Disc Model	14
17	Examples of lines in D^2	15
18	Examples of parallel lines in D^2	16
19	Example of a hyperbolic rotation	17
20	Example of hyperbolic translation	17
21	Example of a hyperbolic reflection	18
22	$4g$ -gon with $g=2$ and associated side-pairings	21
23	Genus- g surface where $g=2$	22

24	Transformation where line l is taken to be the y -axis	23
25	Another transformation of a different line L represented by $\begin{bmatrix} 0 & 1 - .7i & 1 + 7i & 0 \end{bmatrix}$	24
26	Another transformation of a different line L represented by $\begin{bmatrix} 0 & 1 - .3i & 1 + 3i & 0 \end{bmatrix}$	25
27	Transformation using the y -axis and $g=3$	25
28	Another transformation with $g=3$	26

1 Euclidean Geometry

Euclid of Alexandria, Egypt (300 BC), is one of the most famous mathematicians of all time, known for organizing ideas of geometry and founding the axiomatic method, putting mathematics on a firm logical foundation. Euclid taught in Alexandria, Egypt, where many mathematical ideas were initiated, discovered, or discussed. Through involvement in these discussions, Euclid compiled these ideas, theorems, etc., and put them into a collection of works named “The Elements”. In this book, Euclid laid out definitions and terms that were to be taken without proof, and which formed the basis of geometry. Euclidean geometry was originally based on 5 postulates, or statements that are to be taken without proof. From these 5 postulates, all theorems and proofs can be developed. Such a logical progression of ideas remains in use to this day.

Many fundamental ideas form the basis of Euclidean geometry. We consider the Euclidean plane to be the following set: $R^2 = \{(x, y) | x, y \in R\}$, where we define the distance function between two points $P_1 = (x_1, y_1)$ and $P_2 = (x_2, y_2)$ as

$$d(P_1, P_2) = \sqrt{(x_1 - x_2)^2 + (y_1 - y_2)^2}$$

.

If two points are equally distant from a third point, we say they are equidistant (Figure 1).

We can then define a line to be the set of points equidistant from two points. For example, in Figure 1, all points on line L are equidistant from A and B because they are equal distance away from points A and B. The idea of distance allows us to build the idea of isometries, which are distance-persevering maps or functions.

In Euclidean geometry, an isometry of R^2 is defined as a function

$$f : R^2 \rightarrow R^2 \text{ where } d(f(P_1), f(P_2)) = d(P_1, P_2) \text{ for all } P_1, P_2 \in R^2$$

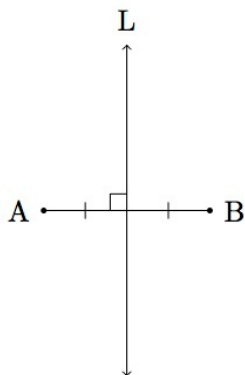


Figure 1: Example of equidistant points

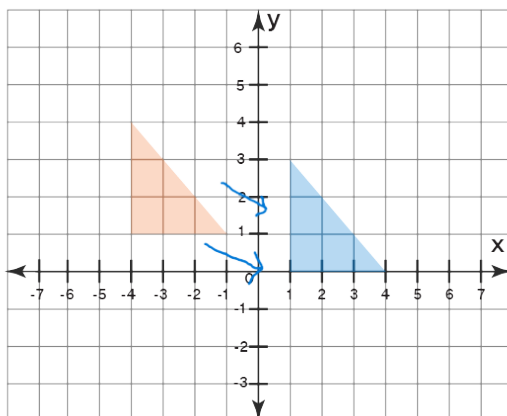


Figure 2: Example of a translation

. Therefore, an isometry preserves the distance between points before and after getting mapped by the isometry.

Euclidean Geometry has 4 types of isometries: translations, reflections, glide reflections, and rotations[4].

A translation moves all points by the same vector. In generic form, we write a translation as $t_{(\alpha, \beta)}$ where $(\alpha, \beta) \in \mathbb{R}^2$ and a point (x, y) is sent to a point (x', y') , where $x' = \alpha + x$ and $y' = \beta + y$. For example, in Figure 2 the orange triangle is translated by a vector to obtain the blue triangle. A translation has no fixed points, however, it has a parallel family of invariant lines (lines that are mapped onto themselves by the isometry), parallel to the

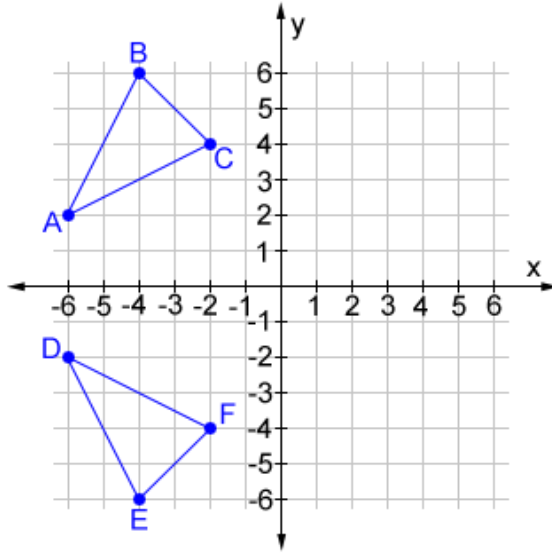


Figure 3: Reflection in the x-axis

vector of translation[4].

A reflection mirrors points over a set line. This leaves the points on the line of reflection as fixed points. The most basic example of a reflection is one over the x-axis, where a point (x, y) is sent to point (x', y') , where $x' = x$ and $y' = -y$ (Figure 3). We write a reflection as \bar{r} .

A rotation rotates points by a specific angle around a specific point, referred to as the center of rotation (Figure 4). This leaves the center of rotation as the only fixed point. We use r_θ to represent a rotation, where θ =the angle of rotation. For a rotation by angle θ around the origin, a point (x, y) is sent to a point (x', y') where $x' = x \cos \theta - y \sin \theta$ and $y' = x \sin \theta + y \cos \theta$.

Finally, a glide reflection is a combination of a translation and a reflection (Figure 5). It reflects a point over a line of reflection and then translates it by a vector parallel to the line. We write it as $t_{(\alpha, \beta)}\bar{r}$, or as $\bar{r}t_{(\alpha, \beta)}$, depending on which isometry is performed first. It is to be noted that when writing a composite of isometries, they are to be done/read from right to left. We note that $t_{(\alpha, \beta)}\bar{r} = \bar{r}t_{(\alpha, \beta)}$.

One can see that every isometry of R^2 is one of these four by using the “three reflections

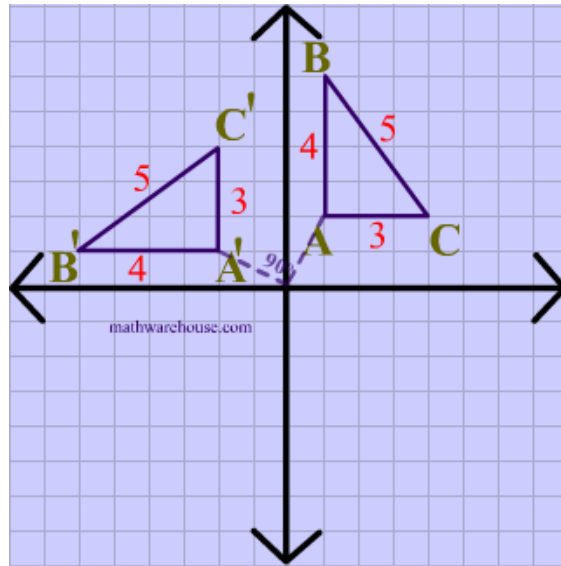


Figure 4: Example of a rotation by 90°

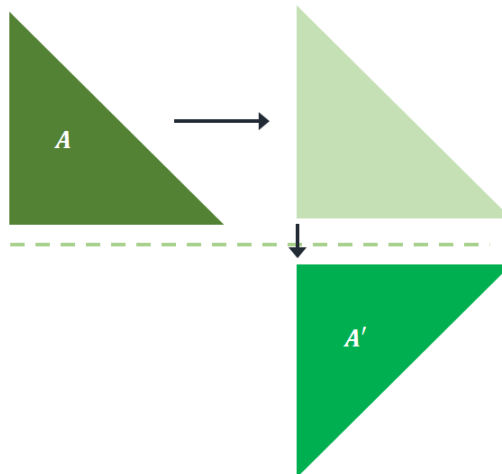


Figure 5: Translation followed by a reflection (also known as a glide reflection)

theorem”[4]. The three reflections theorem states that any isometry f of R^2 is the product of one, two, or three reflections. The reason for this theorem is that any isometry is determined by its effect on three points, that is any isometry f of R^2 is determined by the images $f(A)$, $f(B)$, and $f(C)$ of three points A , B , and C not on a line[4]. Because every composite of three reflections is an isometry of one of the four types listed, it follows that any isometry of R^2 is one of the four types.

It is easy to see that the orientation-preserving isometries will be the product of two reflections (rotations and translations) and the orientation-reversing isometries are the product of one or three reflections (reflections and glide reflections)[4].

Because complex numbers can be identified with points in R^2 , each isometry also has a complex form, which can be very useful when computing certain algebraic expressions with the isometries. First, we denote $z = x + iy$, where $x, y \in R$ and $i \in C$. We view the points $(x, y) \in R^2$ as $z = x + iy \in C$. The following are the formulas for each isometry in complex form:

$$\begin{aligned} t_{(\alpha, \beta)} \text{ becomes } t_{(\alpha + i\beta)}(z) &= \alpha + i\beta + z, & r_\theta \text{ becomes } r_\theta(z) &= e^{i\theta}z \\ \bar{r} \text{ becomes } \bar{r}(z) &= \bar{z}, & t_{(\alpha, \beta)}\bar{r} \text{ becomes } f(z) &= \alpha + i\beta + \bar{z} \end{aligned}$$

Algebraically, many of the proofs and computations become much easier in complex form.

While the above formulas represent several basic isometries, to get rotations around general points or reflections in general lines, we use conjugation. The conjugate of an isometry g by an isometry f is the isometry $f g f^{-1}$. The idea of conjugation is performing the same action but at a different place, or expressing an operation in a new coordinate system[4]. For example, $t_{(\alpha, \beta)} r_\theta t_{(\alpha, \beta)}^{-1}$ translates by the inverse of the translation $t_{(\alpha, \beta)}$, performs the rotation, and then translates the set of points back using a translation. The result is a rotation by θ around point (α, β) . We can now have rotations around a center beside the origin, reflections over other lines besides the x-axis, etc.

2 The Torus and Groups

A group G is defined as a set with an operation \cdot (for $a, b \in G, a \cdot b$ is some element of G that satisfies the following constraints [2]:

- 1) The operation must be associative: for every $a, b, c \in G, a \cdot (b \cdot c) = (a \cdot b) \cdot c$.
- 2) The group G must have a unit element: there exists an element $e \in G$ such that for every $a \in G, e \cdot a = a \cdot e = a$.
- 3) There must exist an inverse element: for every $a \in G$, there is an element $b \in G$ such that $a \cdot b = b \cdot a = e$ (the unit element).

A simple example of a group would be the set of integers Z , with the operation being addition. We can denote this as $(Z, +)$. For all integers a, b , and c , $(a+b)+c=a+(b+c)$ holds, so the associative property is satisfied. 0 is the unit element, as any integer a has the property that $a+0=a$ and $0+a=a$. Also for every integer a , there exists an integer b such that $a+b=0$, where b is simply the opposite of a . Therefore, the set $(Z, +)$ satisfies all the properties of a group.

Specifically, in the scope of geometry, we consider a group G of isometries where the operation is a composition and elements satisfy that the composite of any two elements is in G , and the inverse of any element of G is in G . Take, for example, the group G consisting of translations by integer values in the direction of the x -axis, $t_m(z) = z + m$. First, the operation is composition and it is easy to see that $t_m \circ t_n = t_{m+n}$. If we take some $m, n, o \in Z$, we get that $t_m \circ (t_n \circ t_o) = (t_m \circ t_n) \circ t_o$, as both respectively equal $t_{n+(m+o)}$ and $t_{(n+m)+o}$, which are equal. Therefore, the associative property is satisfied. The unit element is t_0 , as $t_m + t_0 = t_0 + t_m = t_m$. Also, we know $t_m^{-1} = t_{-m}$, so the inverse of each element of the group is in the group. All conditions of the group are satisfied, making G a group. The group G is isomorphic to the example above of the group $(Z, +)$ which means that the groups are essentially the same.

We define the orbit of $x \in R^2$ under a group of isometries Γ to be images of x under all elements of $\Gamma = \{g(x) \mid g \in \Gamma\}$ [4]. We can also denote this as Γx . For example, let

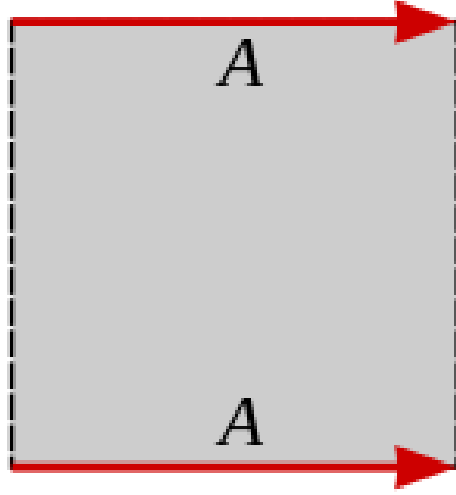


Figure 6: Fundamental polygon of a cylinder with horizontal translations

Γ be the group of horizontal integer translations of R^2 . The Γ -orbit of a point is the set $\{(x + n, y) \mid n \in Z\}$. Next, we will form the quotient space R^2/Γ . For every $x \in R^2$, we will treat its orbit Γx as a single point. Then the quotient space R^2/Γ is the set of orbits, where each orbit is thought of as one element. To understand R^2/Γ better, consider a part of the plane that contains exactly one representative of each Γ -orbit, called a fundamental set. In the above example, the fundamental set is $[0,1) \times R$. A fundamental set is in a bijective correspondence with the quotient space but does not capture the topology of the quotient space. For this, we use the fundamental polygon, a polygon that contains a representative of each Γ -orbit, possibly more than one, but finitely many.

In our above example, $[0,1] \times R$ is an example of a fundamental polygon (Figure 6). Images of this set by all elements of Γ cover the entire plane with overlaps only on the boundary[4].

As another example, a torus can also be formed using a quotient space. We consider the group $\Gamma = \{t_m \vec{e}_1 + n \vec{e}_2\}$ where $m, n \in Z$ and \vec{e}_1 and \vec{e}_2 are basis vectors in R^2 . As stated above, we would like to find a fundamental polygon to better understand R^2/Γ .

The fundamental polygon can be the square $[0,1] \times [0,1]$ (Figure 7).

This group moves this square around the whole plane and all translates will overlap only

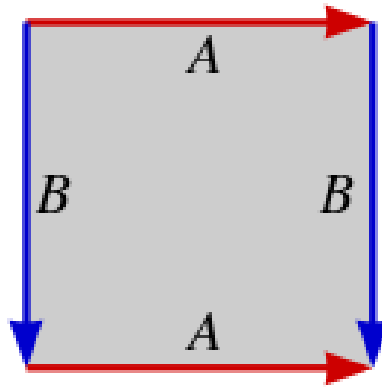


Figure 7: Fundamental region of a torus

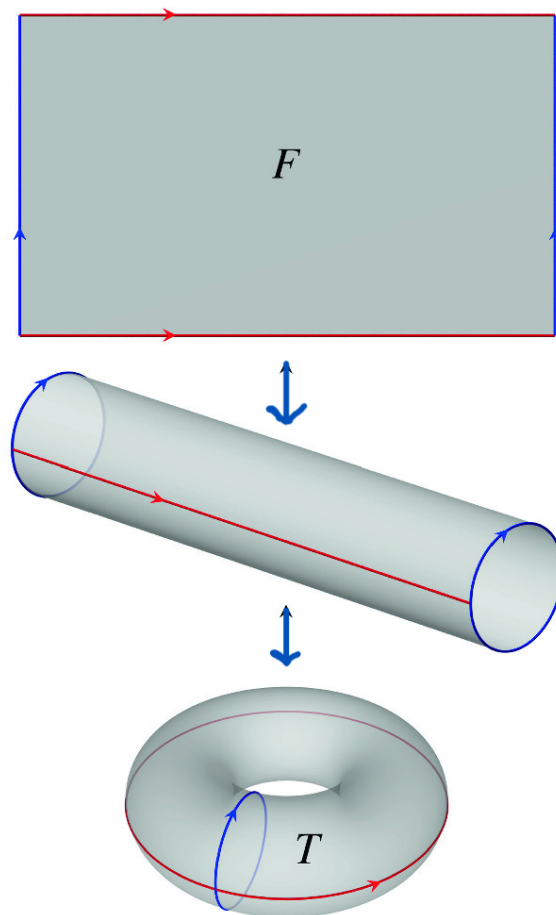


Figure 8: Process of forming a torus from the fundamental polygon

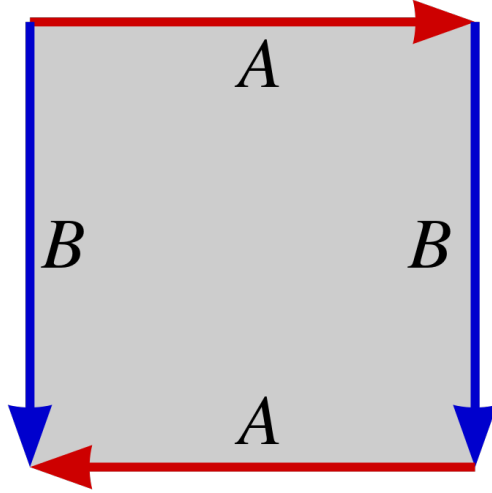


Figure 9: Fundamental polygon of Klein bottle

at the boundary. If we solely look at this square, we see that we can identify the sides because the points on them are in the same orbit. For example, if we take a point Q on the left side of the square and translate it by \vec{e}_1 , we get the point Q on the right side of the square in the same orbit. Therefore, we can identify these sides as they are essentially the same points, which forms a cylinder. Next, we notice that the same can be done with the top and the bottom of the cylinder: if we look back at the original square and take a point Q on the bottom and translate it up by \vec{e}_2 , we get the same point Q on the top. Therefore, we can identify the top of the cylinder with the bottom (Figure 8).

Other notable spaces can be made using this same process of finding a fundamental polyhedron, such as the Mobius strip and the Klein bottle (Figures 9 and 10). A Mobius strip is formed by $\Gamma = \{g^m \mid m \in \mathbb{Z}\}$, where $g = \bar{r} \circ t$. A Klein bottle is formed by $\Gamma = \langle S, t_{\vec{e}_2} \rangle$, where S represents a glide reflection in the x -axis and is shifted by \vec{e}_1 . An example of a fundamental polygon for the Mobius strip is $[0,1] \times \mathbb{R}$, and $[0,1] \times [0,1]$ for the Klein bottle.

A group Γ can have various fundamental polygons. Often they can be intuitively constructed based on our understanding of the group. Here is another way: for example, let

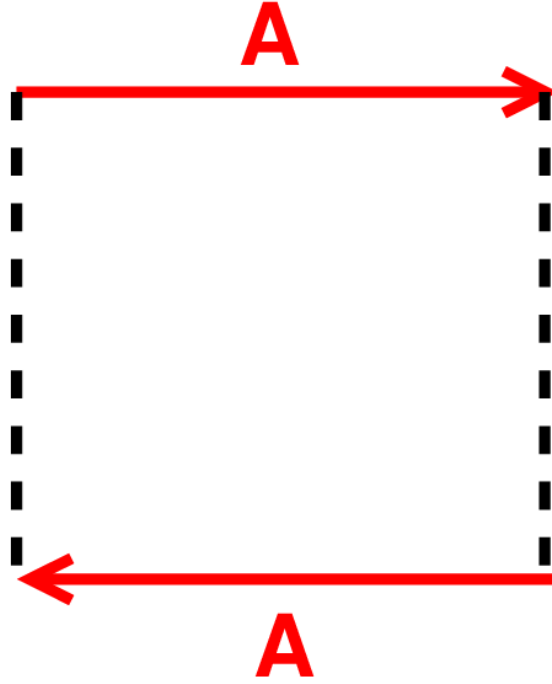


Figure 10: Fundamental polygon of Mobius strip

Γ be generated by the translations t_{e_1} and t_{e_2} , where e_1 and e_2 are the standard basis for \mathbb{R}^2 . If we take the translates of a line, we get a collection of parallel lines. If the line has a rational slope, we get equally spaced parallel lines.

However, if the line has an irrational slope, say $\sqrt{2}$, then we get a dense collection of parallel lines (Figure 11). The term “dense” means that lines become arbitrarily close to each point of \mathbb{R}^2 and fill the plane. The density makes them unsuitable for a fundamental polygon. By using two lines with different rational slopes, we get a grid on the plane and can use several pieces of the grid as a fundamental polygon[4] (Figure 12). We can take lines with rational slopes, for example, $\frac{3}{4}$ and $\frac{1}{2}$, and translate them by all possible translations and we get a picture in which we can find a fundamental polygon for Γ . We also note that distance in \mathbb{R}^2/Γ is defined using distance in \mathbb{R}^2 . More specifically, we can say $d(\Gamma P, \Gamma Q) = \min\{d(P', Q') | P' \in \Gamma P, Q' \in \Gamma Q\}$. The orbit map is the map that sends each $P \in \mathbb{R}^2$ to its orbit $\Gamma P \in \mathbb{R}^2/\Gamma$ and is also denoted as $\Gamma*$, it is a local isometry from the Euclidean plane. $\Gamma*$ is a local isometry where within a certain distance, the geometry of

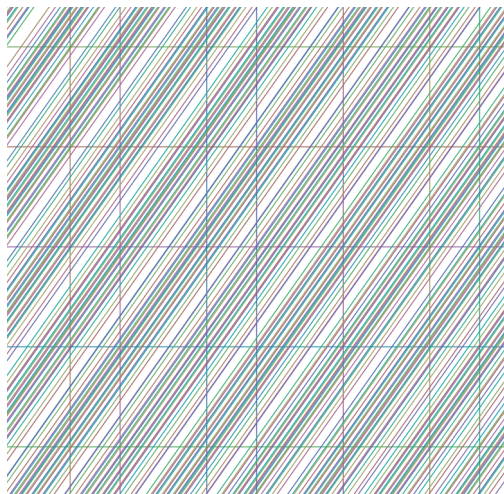


Figure 11: Translates of line with slope $\sqrt{2}$

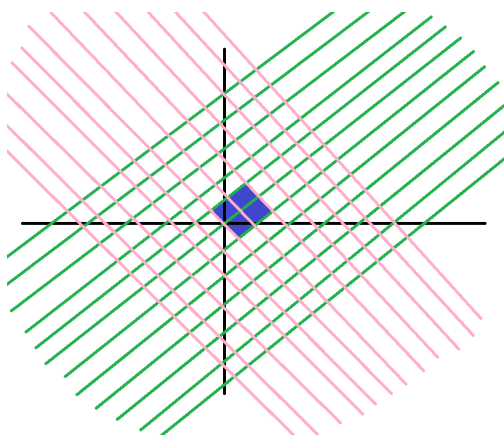


Figure 12: Translations of two lines with rational slope, forming a grid

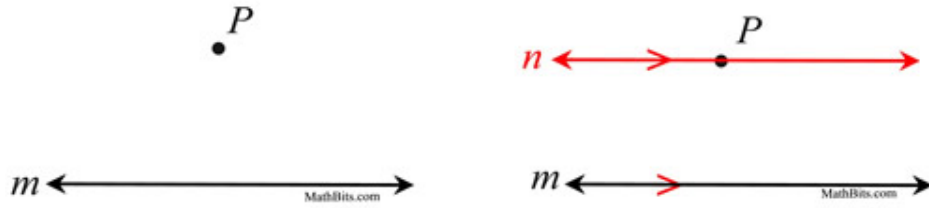


Figure 13: Example of parallel postulate: Point P is not on the line m , and n is the only line going through point P parallel to line m

the quotient space is the same as the geometry of the plane.

Importantly, the kinds of groups we consider are discrete. A discrete group of isometries G is a group of isometries with the additional property of having no limit points[4]. More precisely, we define the term limit point of a subset S of R^2 : x is a limit point of S if every disk around x contains an $s \in S$ such that $s \neq x$. We say Γ is discrete if no point $P \in R^2$ is a limit point of a Γ -orbit. This means that there is a disk around P such that for any orbit ΓQ , there exist no other points of ΓP in the disk, except maybe for P . We also define the term fixed-point free group: Γ is fixed point-free if for every point $P \in R^2$ if $gP = P$, then $g = \text{identity}$. Then a group Γ is discontinuous and fixed point free if and only if every $P \in R^2$ has a neighborhood D in which every point is in a different orbit of Γ , or equivalently, every $P \in R^2$ has a neighborhood D such that $g(D) \cap D = \emptyset$ for all $g \neq 1, g \in \Gamma$. Examples of discrete groups of isometries are all the ones considered above.

3 Hyperbolic Geometry and the D^2 Model

As mentioned earlier, when Euclid wrote “The Elements”, he stated 5 postulates, or statements to be taken without proof, that form the basis of his proofs for numerous theorems. Most of these postulates seem very straightforward and are easy statements to believe without proof. The 5th postulate, however, stood out among the rest for being much more complex. This postulate is also known as the parallel postulate.



Figure 14: Parallel postulate in hyperbolic geometry: Through the point P not on the given line l , there exists two lines, m and n , going through point P parallel to line l

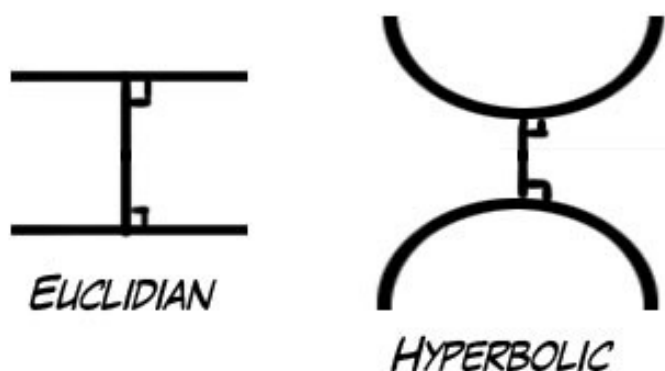


Figure 15: Parallel lines in Euclidean geometry vs hyperbolic geometry

The parallel postulate states that through a point not on a given line, there exists a unique line through that point parallel to the given line (Figure 13). This one did not seem as easy to believe without proof, and for years many mathematicians tried to prove the 5th postulate using the other four and failed. That is because there exist counter-examples of the statement, hyperbolic and spherical geometry. This parallel postulate is what separates Euclidean and hyperbolic geometry.

Euclidean geometry accepts the parallel postulate as written above.

Hyperbolic geometry has the following parallel postulate: through a point not on a given line, there exist multiple lines through that point that are parallel to the given line (Figure 14).

This single difference changes many of the fundamental aspects between the different

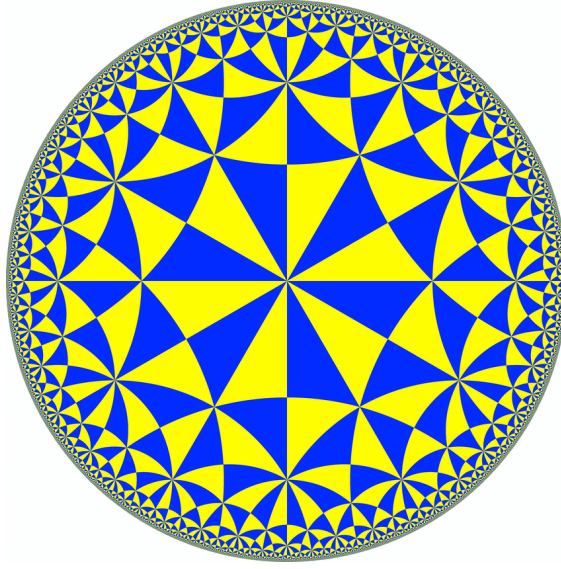


Figure 16: Disc Model

types of geometry. For example, distance.

Hyperbolic geometry is represented by several models, including the half-plane model, disk model, Klein model, etc.

Here, we will be working in the D^2 model, also known as the conformal disc model, or the Poincaré disk model (Figure 16). Visually, the D^2 model is the unit disc, where the disc has a unit radius and is centered as $(0,0)$, so it satisfies the equation $x^2 + y^2 < 1$.

Distance in the D^2 model is defined using lengths of curves. First, for a parametrized curve $\gamma = (x(t), y(t)), t \in [a, b]$, we define $\text{length}(\gamma) = \int_a^b \frac{2\sqrt{x'(t)^2 + y'(t)^2}}{1 - (x(t)^2 + y(t)^2)} dt$. In Euclidean geometry when we talk about distance, without saying it we normally imply that distance is the length of the shortest curve between two points. Hyperbolic geometry has the same property. Between two points a and b , we take distance to be defined as $d(a, b) = \inf \{\text{length of curves connecting } a \text{ and } b\}$, where infimum is the greatest real number that is less than or equal to each element of the set. It can also be thought of as taking the minimum of the set. This setup implies the triangle inequality, because the union of curves γ_1 from P to Q and γ_2 from Q to R is a curve γ from P to R , so $d(P, R) \leq \text{length}(\gamma_1) + \text{length}(\gamma_2)$. Because this holds for any curves γ_1 and γ_2 , it will hold when we take the infimum, hence

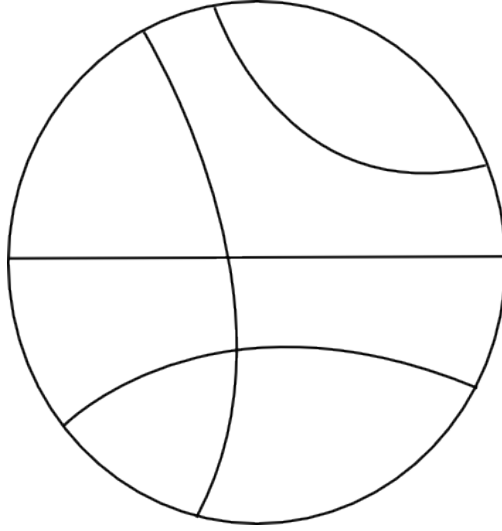


Figure 17: Examples of lines in D^2

$d(P, R) \leq d(P, Q) + d(Q, R)$. It is possible to write a formula for distance between two points in D^2 , but it is much more complicated.

Lines in D^2 are also defined as the set of points equidistant from two points.

In D^2 , hyperbolic lines are either lines through the origin or circles perpendicular to the boundary circle, where we consider only the part inside D^2 (Figure 17).

As mentioned above, parallel lines work differently in the D^2 model.

There exist two types of parallel lines. If the lines intersect at the boundary of the disc, because the boundary of the disc is not a part of D^2 , we say they are parallel and more specifically, that they are hyperparallel or asymptotically parallel[4]. For example, line p is considered hyperparallel to line d in Figure 18, as they only intersect at the boundary. Other parallel lines do not intersect in D^2 nor at the boundary, and these are called disjointly parallel or ultraparallel. For example, line d is considered disjointly parallel to line n in Figure 18.

Just as in Euclidean geometry, isometries exist in hyperbolic geometry as well, defined as distance-preserving maps on the hyperbolic plane. An important aspect of the hyperbolic plane that impacts its isometries is that there exists a natural boundary called the circle

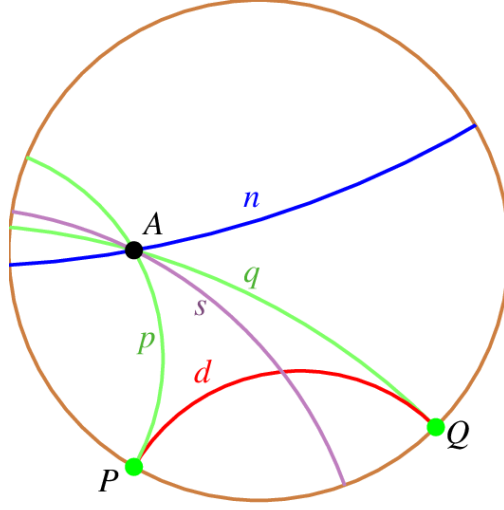


Figure 18: Examples of parallel lines in D^2

at infinity, denoted as ∂D^2 , and is the unit circle. In other words, it is the boundary of D^2 , where the set of points are Euclidean limits of D^2 , but themselves are not in D^2 . For example, in Figure 18, the points P and Q are on the boundary of the disc and therefore not actually in D^2 .

As in Euclidean geometry, hyperbolic geometry isometries include rotations, translations, reflections, and glide reflections, and adds a new isometry, limit rotations. These isometries are most simply expressed in complex form, where $z = x + iy$.

A rotation about the origin in D^2 is given by $r_\theta(w) = e^{i\theta}w$, much like in Euclidean geometry (Figure 19). It has only one fixed point, the center of rotation. It also leaves invariant the circles with center at the origin.

A limit rotation is a “rotation” about a point on the boundary. It moves the lines that go through P, and leaves horocycles invariant. A horocycle is a Euclidean circle in D^2 that touches ∂D^2 . There are no fixed points in D^2 , however, there is one at the circle of infinity, P.

A translation in D^2 along a line l moves points along the line l in one direction and moves other points of D^2 in the direction of the line (Figure 20). The endpoints of the line at the circle at infinity are the only fixed points of a hyperbolic translation and it keeps the line l

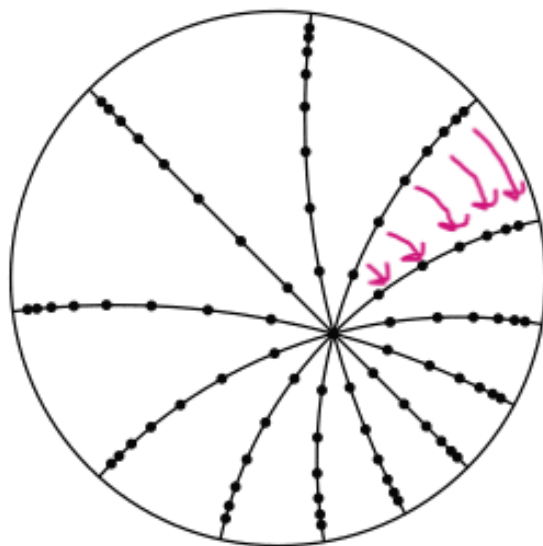


Figure 19: Example of a hyperbolic rotation

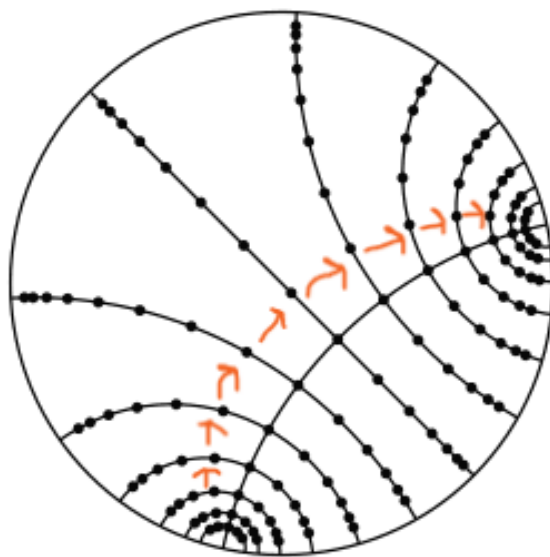


Figure 20: Example of hyperbolic translation

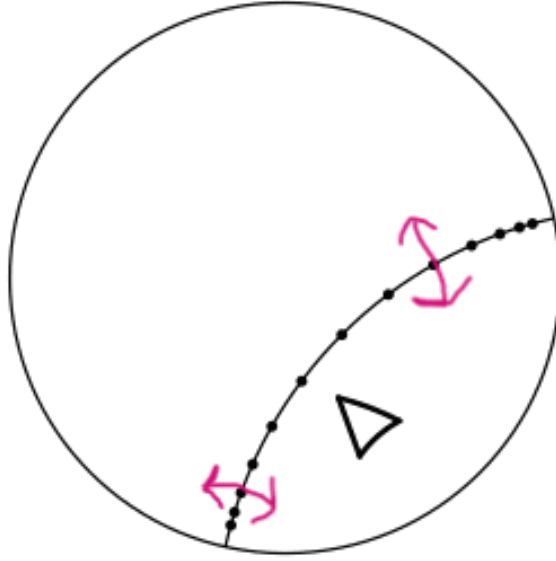


Figure 21: Example of a hyperbolic reflection

invariant.

Hyperbolic reflections in a hyperbolic line l are similar to Euclidean geometry ones. They leave the line of reflection invariant and swap the sides of the hyperbolic line. When the hyperbolic line is a line through the center, it is a Euclidean reflection. When the hyperbolic line of reflection is a circle perpendicular to the boundary, it is an inversion in this circle (Figure 21). If l is a circle in R^2 centered at O and with Euclidean radius r , the inversion $I : R^2 \rightarrow R^2$ is defined as $I(P) = P'$, where P' is on Euclidean line OP and $d(O, P) \cdot d(O, P') = r^2$ [1]. An inversion swaps the inside and outside of the circle l , thereby acting like a reflection in the circle. Lastly, there exist glide reflections, the composite of a reflection in a line with a translation in the direction of the same line.

We can prove the following: the set of points D^2 -equidistant from two points $P, P' \in D^2$ is a D^2 -line and a D^2 -reflection in this line exchanges P and P' . As in Euclidean geometry, we have the three reflections theorem, stating that each D^2 isometry is the product of one, two, or three reflections in D^2 . Also as in Euclidean geometry, we can classify isometries as

orientation-reversing or orientation-preserving. Glide reflections and reflections are the types of isometries in D^2 that are orientation-reversing and therefore is the product of one or three reflections[4]. Translations, limit rotations, and rotations are all orientation-preserving, and therefore the product of two reflections.

As mentioned above, a reflection in a hyperbolic line that is a circle is an inversion in the circle. Because of the three-reflections theorem, all D^2 isometries are products of inversions in circle $C_{\alpha,p}$ or reflections in lines through the origin. Now, we can use the complex form of inversions and reflections to express all D^2 isometries as a complex function of the same form. In complex form, inversions can be written as $i_C(z) = \frac{r^2}{z - z_0} + z_0$, where C represents the circle, z_0 the center and r the radius, and reflections in lines take form $\bar{r}(z) = c + e^{i\theta}\bar{z}$. Using this, we can get all D^2 isometries to be of the form $f(z) = \frac{pz+q}{rz+s}$ if they are orientation-preserving or $\bar{f}(z) = \frac{p\bar{z}+q}{r\bar{z}+s}$, if they are orientation-reversing. Taking into account that inversions are in circles perpendicular to ∂D^2 and reflections are in lines through the origin, we get general forms

$$f(z) = \frac{az+b}{b\bar{z}+\bar{a}} \text{ and } \bar{f}(z) = \frac{a\bar{z}+b}{b\bar{z}+\bar{a}}$$

where $a, b \in C$ and $|a|^2 + |b|^2 = 1$. The first equation represents orientation-preserving isometries in D^2 , while the second equation represents orientation-reversing isometries. Since both of those expressions have form $f(z) = \frac{pz+q}{rz+s}$ or $\bar{f}(z) = \frac{p\bar{z}+q}{r\bar{z}+s}$, and the collection of functions $H = \{z \rightarrow \frac{pz+q}{rz+s}, z \rightarrow \frac{p\bar{z}+q}{r\bar{z}+s} \mid p, q, r, s \in C\}$ is a group, we deduce that every hyperbolic isometry can be written as a complex function from H . Now, there is a map ϕ from 2×2 complex matrices to functions $f(z) = \frac{pz+q}{rz+s}$ given by

$$\phi\left(\begin{bmatrix} p & q \\ r & s \end{bmatrix}\right) = f, \text{ where } f(z) = \frac{pz+q}{rz+s}.$$

The map ϕ satisfies $\phi(AB) = \phi(A) \circ \phi(B)$ (i.e. ϕ is a homomorphism). This allows us to

compute composites of functions by multiplying their corresponding matrices.

We can also represent lines and circles as matrices as well. In complex form, a circle with center d and radius r has the equation $|z - d|^2 = r^2$. A little algebra shows we can write this equation in the form $a|z|^2 + \bar{b}z + b\bar{z} + c = 0$, where $a, c \in R$, $b \in C$, and $|b|^2 - ac \geq 0$. Then, $d = \frac{-b}{a}$ and $r = \frac{\sqrt{|b|^2 - ac}}{|a|}$. Conversely, if $a \neq 0$, every equation $a|z|^2 + \bar{b}z + b\bar{z} + c = 0$ where $|b|^2 - ac \geq 0$ can be written as $|z - d|^2 = r^2$. If in this equation $a = 0$, we get the equation of a line with a normal vector b , so our equation can be used to represent both lines and circles in C . Now, we can write the equation in matrix form as follows:

$$\begin{bmatrix} a & b \\ \bar{b} & c \end{bmatrix} \begin{bmatrix} z \\ 1 \end{bmatrix} \cdot \begin{bmatrix} \bar{z} \\ 1 \end{bmatrix} = 0$$

where \cdot is the dot product of vectors, so a matrix with a negative determinant can be used to represent a line or circle. Note, if $A = \begin{bmatrix} a & b \\ \bar{b} & c \end{bmatrix}$ represents a circle, then its radius is $\frac{\sqrt{-\det A}}{|a|}$. We can also find the image of a line or circle L by the function $f(z) = \frac{pz+q}{rz+s}$ as follows: if matrix A corresponds to L and matrix F corresponds to f and matrix F^* is the conjugate transpose of matrix F , then matrix F^*AF corresponds to $f^{-1}(L)$ [3].

4 $4g$ -gon and the Genus- g Surface

A polygon in D^2 is, just like in R^2 , a region of D^2 bounded by hyperbolic lines. In the D^2 model, there exists a symmetric polygon with $4g$ sides called the $4g$ -gon.

Just like the side-pairings of a parallelogram in R^2 that produce a torus, there is a side-pairing of the $4g$ -gon that produces an interesting space. To understand a simpler example, take $g=2$. We get an octagon in D^2 (figure 22). We can take a line through the center and two

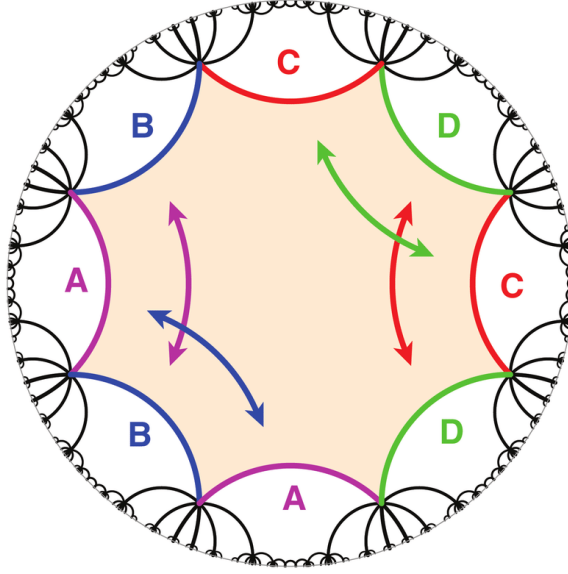


Figure 22: $4g$ -gon with $g=2$ and associated side-pairings

vertices, and divide this octagon into two pieces, each with 4 sides from the original octagon, and the fifth from dividing it. The 4 sides can be paired by two hyperbolic translations. Then, much as we did with a torus, we can “glue” the paired sides. Note that each of the pieces has a side-pairing just like the side pairing of a square that produces a torus, but the 5th side is not identified with anything, so we see the result of side pairing is a torus with a hole.

Since each of the pieces of the octagon produces a torus with a hole, and their unpaired fifth sides need to be identified, we glue the holes together and form what is known as a genus-2 surface (Figure 23). In the name, g represents the number of toruses that compose the overall surface. If we, for example, consider $g=3$, then the $4g$ -gon is a 12-sided symmetric polygon in D^2 with a similar side pairing; 3 blocks of 4 adjacent sides are paired in a similar way by hyperbolic translations. The result of identification at the sides is a genus-3 surface that has 3 “holes” connected. The isometries that produce these side-pairings form a discrete group which we denote here as Γ , because the side-pairings satisfy certain technical conditions.



Figure 23: Genus- g surface where $g=2$

The purpose of this research is to take this group and apply the isometries from it to a chosen hyperbolic line in D^2 in order to determine if the images of L form a dense set. If not, then we may be able to construct a fundamental polygon using images of several hyperbolic lines, like in section 2 for the group of translations of R^2 .

5 Computation Setup

To carry out the research, we used the computer application Mathematica, which allows easy use of matrix computations and graphing. To begin, we first computed our first side pairing f_1 by hand: it is the composite of an inversion in one side and a reflection in a line that sends a side to the paired side. Because the other side-pairing pattern is simply a rotation of one-side-pairing, we conjugated f_1 by rotations to get all generators f_1, f_2, \dots, f_{2g} . We computed with matrices which we stored in a list along with their inverses. We also chose a line to transform with isometries in Γ and represented it with matrix A . Using the formula F^*AF , we computed the images of the line by each of the generators and their inverses and stored the results in a list. We then ran the same process for each element of the new list to obtain a new list of images by composites of the two generators or their inverses. So each

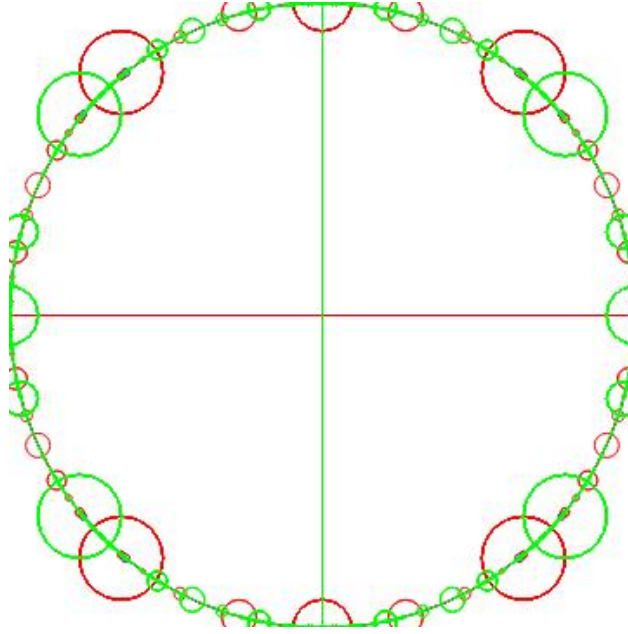


Figure 24: Transformation where line l is taken to be the y -axis

iteration gave exponentially more images of the line (factor= $2g$). For $g=2$, the list grew from 8 to 64 to 512, etc. Because our main goal is to visually see if these transformations produce dense lines we graphed all of the images formed in one iteration over the unit circle. We then saved the picture from each iteration and overlayed all the pictures to see the lines produced. For each starting line we chose, we were only able to run 5 iterations of the transformation or fewer before Mathematica reached its capacity. It is to be noted that throughout this process, there are some repetitions of the same line, but it is not a large proportion.

6 Results

The first line we tested was the y -axis. This seemed like it would give a good starting point, as other theory implies we would get images that are not dense. From the figure, we see the resulting transformation of the y -axis produces a clean picture. Only two lines go through the center, and the rest of the lines appear as half-circles along the boundary of the unit circle. Therefore, we see there are no dense lines from this transformation.

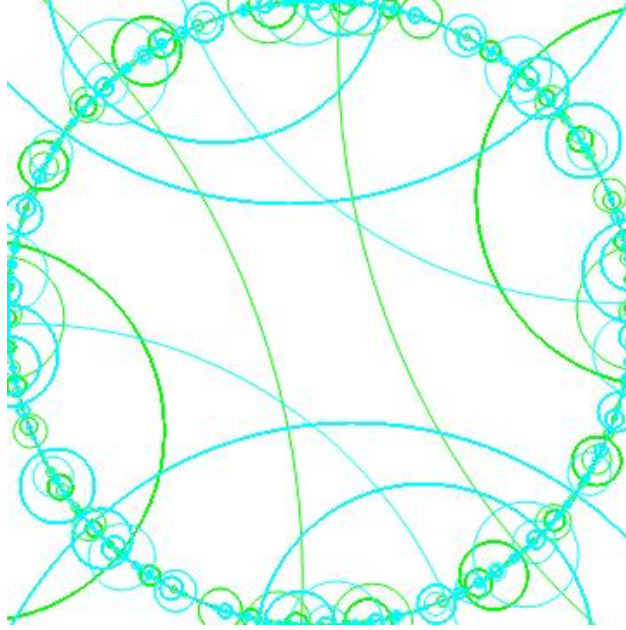


Figure 25: Another transformation of a different line L represented by $\begin{bmatrix} 0 & 1 - .7i \\ 1 + 7i & 0 \end{bmatrix}$

We noticed that every two iterations of our loop produces the original line on the graph. This is because every two iterations produce $f_p^{-1}(f_p(L)) = L$, where $p = 1, 2, \dots, 2g$. In other terms, every two iterations we will have applied a generator f_p to L in the first iteration and then the generator f_p^{-1} to its image in the second iteration, getting $f_p^{-1}(f_p(L)) = L$. This gave us more confidence in the correctness of our images and is an example of repeated lines in the list. In general, $\frac{1}{4g}$ of the items in the list after two iterations are items from the original list, but the list grows by factor $(4g)^2$ after two iterations.

Next, we took the lines represented by matrixes: $\begin{bmatrix} 0 & 1 - .7i \\ 1 + 7i & 0 \end{bmatrix}$ and $\begin{bmatrix} 0 & 1 - .3i \\ 1 + 3i & 0 \end{bmatrix}$ and obtained the following images of Figures 25 and 26.

We see some larger circles are close to the center but there is still no density at the center.

As stated above, we can take g to be any integer to form the genus- g surface. Because of this, we also tried transformations where g was 3 and 4.

We took $g=3$ and line L to be the y -axis. As Figure 27 shows, the lines become very dense and chaotic towards the boundary of the unit circle, however leaves the center of the

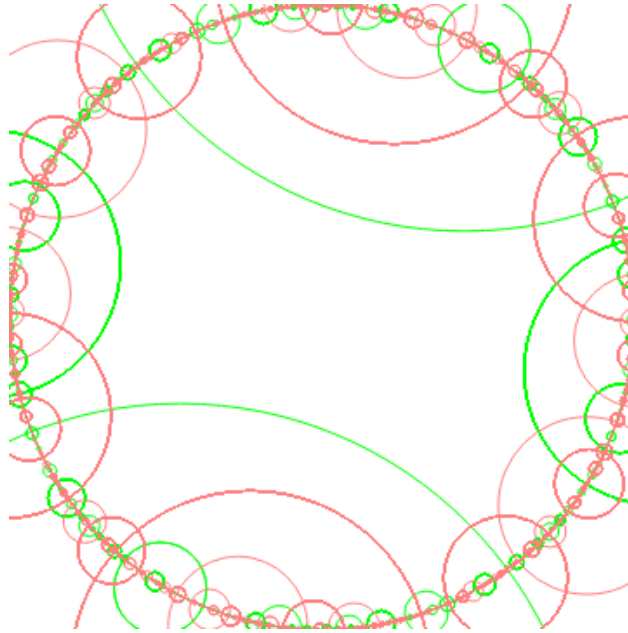


Figure 26: Another transformation of a different line L represented by $\begin{bmatrix} 0 & 1 - .3i \\ 1 + 3i & 0 \end{bmatrix}$

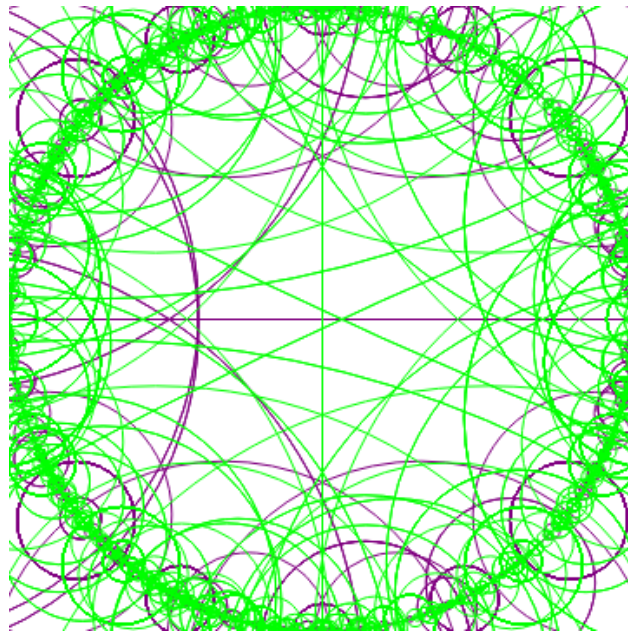


Figure 27: Transformation using the y -axis and $g=3$

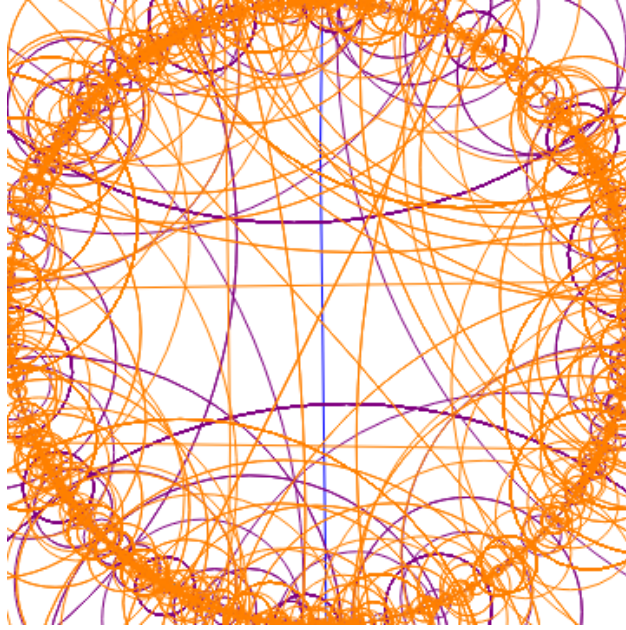


Figure 28: Another tranformation with $g=3$

disk not dense. This was only using 4 iterations.

Inspired by our first results, we decided to run more transformations where $g=3$. We used matrix $\begin{bmatrix} 0 & 1 - .5i \\ 1 + 5i & 0 \end{bmatrix}$ and obtained the image shown in Figure 28.

Again, similar to Figure 27, we notice that after 4 iterations, we see density around the boundary of our unit circle.

7 Conclusion

From our results, we see that if we start with a line through the origin, we always get a nice picture that suggests no density. It is to be noted, however, that Mathematica's capacity only goes up to 5 iterations before it times out. This means we are only seeing images of L by isometries of Γ that are products of up to 5 generators. Since a general isometry of Γ can be a product of any finite number of generators it is possible that images by some of the unexplored isometries may be dense. A possible solution to the problem could be to take a random collection of generators and apply them to line L to get the image L' and the initial

line in our process, and repeat the above process to line L' as the starting line. If we take a random collection of 15 generators and apply them to L to get L' and run the process up to 5 iterations, we would get images of lines by up to 20 generators.

As stated earlier, hyperbolic lines can also appear as circles in the D^2 model. We attempted circles as lines to transform, however, Mathematica had difficulty in graphing the results. We believe that because a transformation over a circle in the D^2 model has a higher chance of producing more complex matrices, Mathematica struggles to graph these complex matrices, and its capacity is reached much earlier, as early as the second iteration, perhaps due to rounding errors.

Overall, this research gives some reason to believe that the transformation of lines in the D^2 model does not produce dense lines, and may be used to construct a fundamental polygon.

References

- [1] Boris N. Apanasov. *Conformal geometry of discrete groups and manifolds*, volume 32 of *De Gruyter Expositions in Mathematics*. Walter de Gruyter & Co., Berlin, 2000.
- [2] Thomas W. Hungerford. *Algebra*, volume 73 of *Graduate Texts in Mathematics*. Springer-Verlag, New York-Berlin, 1980. Reprint of the 1974 original.
- [3] Junehyuk Jung and Alan W. Reid. Embedding closed totally geodesic surfaces in bianchi orbifolds, 2020.
- [4] John Stillwell. *Geometry of surfaces*. Universitext. Springer-Verlag, New York, 1992.

References for Figures

(2016). Points equidistant from two points in the plane. photograph, Illustrative Mathematics. <https://tasks.illustrativemathematics.org/content-standards/tasks/967>. Accessed 20 April 2024.

Transformations. Cuemath. <https://www.cuemath.com/geometry/transformations/>. Accessed 20 April 2024.

(2024b). Reflection. Math.net. <https://www.math.net/reflection>. Accessed 21 April 2024.

Diagram 3. What is an Isometry? Math Warehouse. <https://www.mathwarehouse.com/transformations/what-is-an-isometry.php>. Accessed 20 April 2024.

(2023). Glide Reflection- Definition, Process, and Examples. Story of Mathematics. <https://www.storyofmathematics.com/gilde-reflection/>. Accessed 20 April 2024.

(2014). Fundamental Polygon. Wikimedia Commons. https://commons.wikimedia.org/wiki/Fundamental_polygon. Accessed 21 April 2024.

(2024). Fundamental Polygon. Wikipedia. https://en.wikipedia.org/wiki/Fundamental_polygon. Accessed 20 April 2024.

Stillwell, J. (2020). Fig. 15.5. Topology. Springer Link. <https://link.springer.com/chapter/10.1007/978-3-030-55193-315>. Accessed 20 April 2024.

(2023). Solid Torus. Wikipedia. https://en.wikipedia.org/wiki/Solid_torus. Accessed 20 April 2024.

Pigazzini, A., Pincak, R., Jafari, S., Ozel, C., D & DeBenedictis, A. (2021). Figure 2. A topological approach for emerging D-branes and its implications for gravity (accepted for publication in “International Journal of Geometric Methods in Modern Physics”). ResearchGate. https://www.researchgate.net/publication/353878853_A_topological_approach_for_emerging_D-branes_and_its_implications_for_gravity_accepted_for_publication_in_International_Journal_of_Geometric_Methods_in_Modern_Physics?_tp=eyJjb250ZXh0Ijp7ImZpcnN0UGFnZSI6Il9kaXJlY3QiLCJwYWdlIjojX2RpcmVjdCJ9fQ. Accessed 20 April 2024.

Yamagishi, Y. (2011). Figure 2. Stripes on Rectangular Tilings. ResearchGate. https://www.researchgate.net/publication/48188463.Stripes_on_rectangular_tilings?_tp=eyJjb250ZXh0Ijp7ImZpcnN0UGFnZSI6Il9kaXJlY3QiLCJwYWdlIjoieX2RpcmVjdCJ9fQ. Accessed 20 April 2024.

Roberts, D. The Parallel Postulate. MathBitsNotebook. <https://mathbitsnotebook.com/Geometry/ParallelPerp/PPparallelPostulate.html>. Accessed 20 April 2024.

Bishop, W. 3.1: Hyperbolic Geometry. LibreTexts Mathematics. https://math.libretexts.org/Bookshelves/Geometry/Modern_Geometry_28Bishop29/033A_Introduction_to_Hyperbolic_Geometry/3.01A_Hyperbolic_Geometry. Accessed 20 April 2024

(2014). Non-Euclidean Geometry Art. Harrison's Hartle's Art/Music/Theater F200 Blog. <https://harrisonhartle.wordpress.com/2014/08/04/non-euclidean-geometry-art/>. Accessed 20 April 2024.

Von Gagern, M. (2014). Figure 2. Creation of Hyperbolic Ornaments – Algorithmic and Interactive Methods. ResearchGate. https://www.researchgate.net/figure/A-pattern-in-the-Poincare-disk-model_fig1_291808218. Accessed 20 April 2024.

Figure 1. The Poincare disk model for the hyperbolic plane. Cornell. <https://pi.math.cornell.edu/mec/Winter2009/Mihai/section7.html>. Accessed 20 April 2024.

Margenstern, M. (2009). Figure 1. About a new splitting for the algorithmic study of the tilings $\{p, q\}$ of the hyperbolic plane when q is odd. ResearchGate. https://www.researchgate.net/figure/Illustration-of-the-parallel-axiom-of-hyperbolic-geometry-The-lines-p-and-q-are-the_fig1_45885641. Accessed 20 April 2024.

Jerdonek, C. Hyperbolic Plane Isometry. Encycla. https://encycla.com/Hyperbolic_plane_isometry. Accessed 20 April 2024.

Goldman, W. M. (2012). Figure 2. a Projective Structure? ResearchGate. https://www.researchgate.net/figure/The-fundamental-octagon-is-realized-geometrically-by-a-regular-octagon-in-the-Poincare_fig4_265740969. Accessed 20 April 2024.

(2024). Genus (mathematics). Wikipedia. https://en.wikipedia.org/wiki/Genus_28mathematics29.

Accessed 20 April 2024.